

## MICROWAVE ELECTROMAGNETIC SHIELDING EFFECTIVENESS OF $\text{ZnNb}_2\text{O}_6$ -CHOPPED STRANDS COMPOSITES FOR RADAR AND WIDEBAND (6.5–18 GHz) APPLICATIONS

E.İ. Şahin

*Advanced Technology Research and Application Center, Adana Alparslan Türkeş Science and Technology University,  
Adana 01250, Turkey  
Email: shnethem@gmail.com*

Received 14 June 2022; revised 9 September 2022; accepted 12 September 2022

In this study, the traditional mixed oxide process was used to create  $\text{ZnNb}_2\text{O}_6$ -chopped strands composites. The single phase compound with the chemical formula  $\text{ZnNb}_2\text{O}_6$  was generated after sintering at 1100°C for 4 h. For the structural investigation, various quantities of  $\text{ZnNb}_2\text{O}_6$ -chopped strands were generated. X-ray diffraction (XRD), scanning electron microscopy (SEM) and energy-dispersive X-ray spectroscopy (EDS) were carried out for the structural analysis, which indicated that the second phase did not form in  $\text{ZnNb}_2\text{O}_6$ . Additionally, the  $\text{ZnNb}_2\text{O}_6$ -strands composites were manufactured by hot pressing using the compositions of  $\text{ZnNb}_2\text{O}_6$ -chopped strands in various proportions and epoxy. The  $\text{ZnNb}_2\text{O}_6$ -chopped strands compound formed in various weights, and epoxy resin were used to fabricate microwave shielding effectiveness composites. Utilizing a network analyzer, the microwave shielding effect of  $\text{ZnNb}_2\text{O}_6$ -chopped strands composites was investigated in a range of 6.5–18 GHz. At a thickness of 1.5 mm, a minimum of –51.32 dB shielding effectiveness value was achieved at 6.75 GHz. The  $\text{ZnNb}_2\text{O}_6$ -chopped strands compounds were produced as composite and their features were characterized for shielding effectivity. The content of components in the samples may be managed for the larger and needed frequency bands to change the microwave shielding performance.

**Keywords:** microwave shielding,  $\text{ZnNb}_2\text{O}_6$ , mixed oxide, chopped strands, matrix composites

### 1. Introduction

Electromagnetic interference (EMI) is growing with the abundance of electronic equipment. Technological devices can be affected to a large degree by the signal radiation caused by EMI [1, 2]. Because of the increase in demand for high frequency applications in the radar, satellite communications, and mobile communication sectors, electromagnetic radiation and electromagnetic interference are currently viewed as a serious threat [3]. EMI might be caused by a variety of reasons, including radio transmitters, antennas and lightning, which all produce in the far field [4]. Radiations created by EMI can harm the electronic applications to a large degree. The effects of these EMIs are disturbances in radio or video signals while a plane is flying at low altitudes. This can cause the digital machines

to malfunction at high exposure and also impact people's health [5, 6].

Besides there is a growing concern about harmful effects on human health of electromagnetic (EM) radiation, especially from future (5G) communication systems [7]. Providing a shield that filters interference is the just option for preventing harmful radiation and shielding electronic equipment. The shielding materials of solid and light weight is in high interest [8–10]. Through reflection or absorption of radiation power, EM shielding materials reduce interference by converting EM energy into thermal energy [11]. The best shielding material should have a good electrical conductivity, perfect thermal conductivity and a high EMI shielding effect value [12, 13]. Reflection and absorption of EM waves is predicated on the impedance matching of the medium in

free space and the medium owing to the material. Shielding reduces the interaction between electromagnetic, electrostatic and wave fields. This behaviour is affected by the matter utilized, the shield thickness, the duration and frequency of fields of interest and the aperture orientation in a field to an incidence EM field [14, 15]. Shielding effective materials can be made more efficient by integrating dielectric grains into them, enabling the shielding material thickness decrease, another method is the absorption/reflection of radiation by specific polymeric/metallic shielding materials placed near radiating components for electromagnetic interference shielding (EMIS) [16, 17]. Shielding effective materials are utilized as blockers to reduce the electromagnetic field in space by blocking the fields, for instance, shielding of radio frequency is usually the means of preventing radio waves and radiation [18].

Microwave dielectric materials are in great demand due to rapid improvements in microwave communication.  $\text{ZnNb}_2\text{O}_6$  ceramics are gaining popularity because of their excellent dielectric microwave properties, low sintering temperature and inexpensive cost. The dielectric constant of the columbite-structured  $\text{ZnNb}_2\text{O}_6$  compound is 25,  $Qxf$  (quality factor and resonant frequency) is 83.700 GHz, and the temperature coefficient of resonant frequency is  $-56 \text{ ppm}/^\circ\text{C}$  [19–21]. In the columbite structure,  $\text{ZnNb}_2\text{O}_6$  (zinc niobates) is a low loss dielectric material with an excellent dielectric permittivity, a higher quality factor and a low temperature resonant frequency coefficient. The temperature of zinc niobate sintering is relatively low ( $\sim 1200^\circ\text{C}$ ). Therefore, it is also commonly utilized in microwave communication tools as dielectric resonators [22].  $\text{ZnNb}_2\text{O}_6$  nano ceramics may be fabricated using a variety of processes, including solid state sintering and reaction sintering [23, 24]. Composite materials are made up of a mixture of two or more micro components that are insoluble in each other and have various forms. In the high-performance composite fabrication industry, glass fibres (glass fibre roving or chopped strands) are amongst the most significant reinforcements with excellent mechanic features in high performance composite fabricating industries [25]. Glass fibre is a cost-effective and all-purpose reinforcement for composites. It is corrosion-resistant and lightweight. The quali-

ties of the composite are determined by the interface connection between the glass fibres and the matrix resin [26]. The mat of chopped strands because of its perfect strength, moisture resistance, and electric and fire insulation compared to other composites, e-glass/epoxy composites, is also emerging as a potential material for maritime applications. Chopped strands are chopped from continuous glass fibres. The chopped strands are designed to resist the rigours of compounding. Owing to their upper profile physical and chemical properties, they are mostly used in the production of technical textiles such as automotive textiles, sports textiles, in the aviation sector, wind turbine blades and textile reinforcement concrete [27]. In the previous research, the colemanite/PANI/ $\text{SiO}_2$  composites were measured, and their maximal electromagnetic shielding performance was  $-41.1 \text{ dB}$  at 16.09 GHz at a thickness of 1.5 mm [28]. T-ZnO@Ag/silicone rubber composites were also tested for the electromagnetic shielding effect with 2 mm rubber layers [29]. The produced graphene nanocomposites were shown to have a shielding effect value of  $-30 \text{ dB}$  in the X-band in another study [30]. Furthermore, 0.25% multi-walled carbon nanotube (MWCNT) composites had the highest electromagnetic shielding effectiveness of  $-39 \text{ dB}$  at 1.6 GHz [31]. The capacity of the shielding effect is proportional to how far the incoming electromagnetic wave goes through the material. It is widely acknowledged that when the shielding effectiveness is  $-10 \text{ dB}$ , the entering electromagnetic wave is reduced by 90% while 10% passes to the opposite side [32, 33].

In this investigation, the  $\text{ZnNb}_2\text{O}_6$ -chopped strands were generated as a composite according to optimal parameters, and their shielding effectiveness properties were established. New composites were produced using epoxy at various proportions and  $\text{ZnNb}_2\text{O}_6$ -chopped strands were formed at different proportions by hot pressing. XRD (Bruker/Alpha-T) was used to determine these composites that were characterized. The microwave shielding effectiveness of  $\text{ZnNb}_2\text{O}_6$ -chopped strands composites was measured with a N 5230A PNA series network analyzer (Agilent Technologies) device that was able to measure EMI-SE in the 10 MHz–40 GHz frequency range, including certain radar frequency bands.

## 2. Experiment

### 2.1. Preparation of $\text{ZnNb}_2\text{O}_6$

The mixed oxide process was used to create  $\text{ZnNb}_2\text{O}_6$  powder. ZnO (99.9%) was obtained from *Merc* powders, whereas  $\text{Nb}_2\text{O}_5$  (*Sigma-Aldrich*: 99%) was obtained from *Sigma-Aldrich* powders. Powders of ZnO and  $\text{Nb}_2\text{O}_5$  were mingled in a stoichiometric ratio. Ball milling was employed to mix powders for 20 h, then zirconia balls were utilized to increase the mixture even more. To avoid evaporation losses, the slurries were dried at 100°C for 20 h before being calcined at 600°C for 4 h in a hermetically sealed alumina crucible. The slurries were tested by weighing the specimens before and after calcination. The calcined powders were crushed in an agate mortar and sintered for 4 h between 1000 and 1200°C. After calcining at 600°C, the single-phase  $\text{ZnNb}_2\text{O}_6$  powders were sintered at 1100°C. X-ray diffractometry (XRD-D2 Phaser *Bruker* AXS) was employed on the Cu-K $\alpha$  radiation ( $\lambda = 1.5406 \text{ \AA}$ ) in the range  $2\theta$ : 10–70° at a scan rate of 1°/min to characterize the phases in sintered  $\text{ZnNb}_2\text{O}_6$ . To observe the phases, a scanning electron microscope (*JEOL* 5910LV) was utilized to examine the microstructure and morphology of the samples. To increase conductivity, powder samples were put on a carbide tape and coated with Au/Pd alloy. The chemical analysis was carried out using dispersive spectrometry (EDS, *Oxford-Inca-7274*). The microwave shielding effects of the  $\text{ZnNb}_2\text{O}_6$ -chopped strands composite materials were determined in a range of 6.5–18 GHz using a N 5230A PNA series network analyzer device (*Agilent Technologies*).

### 2.2. Preparation of $\text{ZnNb}_2\text{O}_6$ -chopped strands composites

After being pulverized in an agate mortar, the chopped strands were mingled in stoichiometric proportions with sintered  $\text{ZnNb}_2\text{O}_6$  powders. Powders were mingled in ethanol in a plastic container for 20 h at 20–80 and 40–60 wt.%, respectively, according to the chopped strands – sintered  $\text{ZnNb}_2\text{O}_6$  compositions in the ethanol medium. Ball milling was employed to swirl particles in an ethanol medium within a plastic container for 20 h, then zirconia balls were utilized to increase

the mixture even further. The slurries were dried for 20 h at 100°C, the composites were acquired by filtering and washing the resultant mixture with deionized water and ethanol, then dried under vacuum for 24 h at 60°C for press. The characteristics of electromagnetic shielding efficacy of composites with varied molar ratios were investigated. The  $\text{ZnNb}_2\text{O}_6$ -chopped strands composites with different ratios (strands –  $\text{ZnNb}_2\text{O}_6$  (at 20–80 wt.%), strands –  $\text{ZnNb}_2\text{O}_6$  (at 40–60 wt.%)) were manufactured to see how the strands constituent affected the electromagnetic shielding effect. The composites were made using chopped strands and  $\text{ZnNb}_2\text{O}_6$ . Hot pressing was used to create  $\text{ZnNb}_2\text{O}_6$ -chopped strands composites in varied ratios.

### 2.3. Preparation of epoxy-( $\text{ZnNb}_2\text{O}_6$ -chopped strands) composites

$\text{ZnNb}_2\text{O}_6$ -chopped strands composition powders and epoxy were moulded and cured to create the composites. The specimen powders were mixed with epoxy in a 5:1 weight ratio. Moulding was done in a hydraulic press at 5 MPa pressure and 150°C for 1 h. To evaluate the shielding effect, they were formed into pellets with a diameter of 20 mm and a thickness of 1.5 mm. Composites were fabricated using epoxy in certain ratios of  $\text{ZnNb}_2\text{O}_6$ -chopped strands to provide a broadband microwave shielding effect.

## 3. Results

### 3.1. XRD analysis of $\text{ZnNb}_2\text{O}_6$ -chopped strands

To characterize the  $\text{ZnNb}_2\text{O}_6$  and chopped strands, the X-ray diffraction pattern was analysed. The XRD study of  $\text{ZnNb}_2\text{O}_6$  annealed at 1100°C for 4 h demonstrated the formation of a single phase structure, as well as chopped strands (Fig. 1). Principal phases are designated as  $\text{ZnNb}_2\text{O}_6$ , as can be observed in the detection of  $\text{ZnNb}_2\text{O}_6$  XRD analysis (Fig. 1, PDF Card No. 01-076-1827). The single phase construction of powders was achieved by employing mixed oxide synthesis with the appropriate calcination temperature and the elimination of any possible intermediary phases. All of the specimens were sintered for 4 h at 1100°C. The powders for  $\text{ZnNb}_2\text{O}_6$  did not have

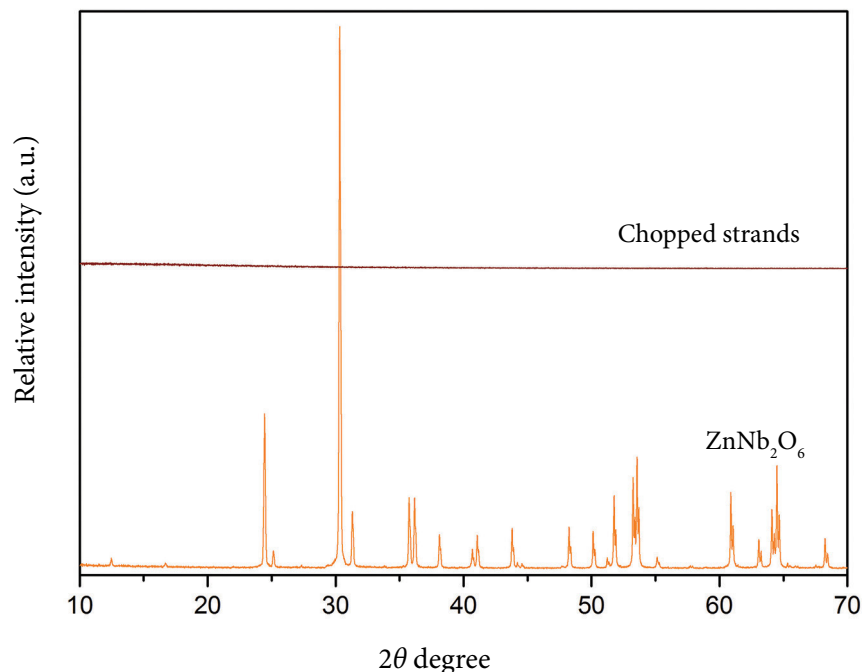


Fig. 1. X-ray powder diffraction patterns of single phase  $\text{ZnNb}_2\text{O}_6$  sintered for 4 h at  $1100^\circ\text{C}$ .

a secondary phase, according to XRD examination. The diffraction peaks of samples were compatible with  $\text{ZnNb}_2\text{O}_6$ -chopped strands and their phase structures remained single phase  $\text{ZnNb}_2\text{O}_6$ -pure chopped strands phase.

Furthermore, the synthesis of  $\text{ZnNb}_2\text{O}_6$  is mainly temperature dependent, and high temperatures are occasionally used to produce single phases.

### 3.2. SEM analysis of $\text{ZnNb}_2\text{O}_6$

The specimens sintered at  $1100^\circ\text{C}$  for 4 h were investigated using SEM.

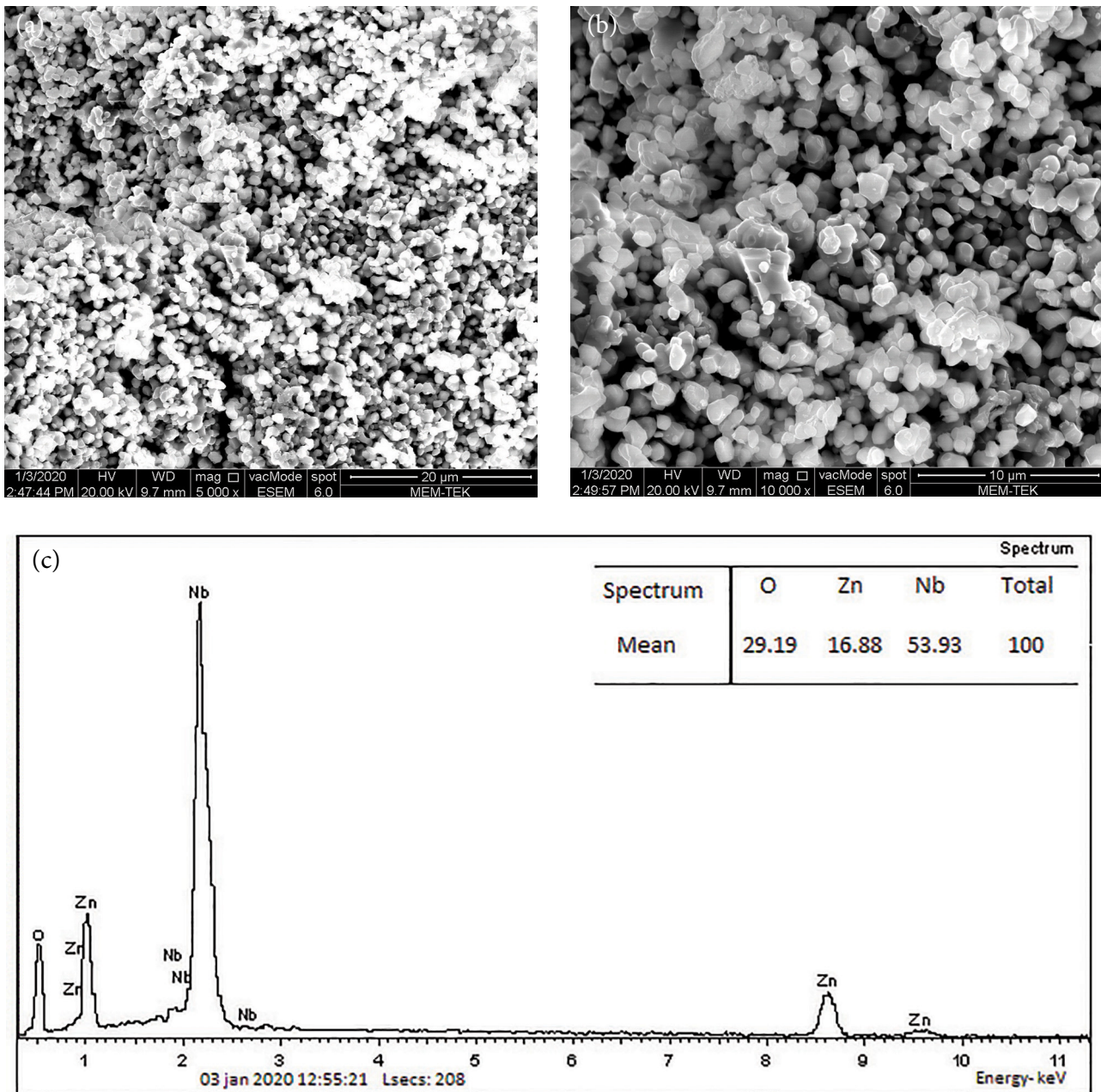
As suggested by the XRD analysis, the SEM analysis showed that only a  $\text{ZnNb}_2\text{O}_6$  single-phase structure was formed in all samples, and no secondary phase or impurity in the microstructure was found (Figs. 2(a, b)).

It was observed that grains with morphology compatible with each other were formed in the microstructure. Most grains have a spherical shape, no significant difference in composition was observed between grains with different morphologies in the EDS analysis. The results of the EDS analysis applied to the  $\text{ZnNb}_2\text{O}_6$  grains gave results very close to the theoretical  $\text{ZnNb}_2\text{O}_6$  composition (16.8% Zn, 53.9% Nb, 29.1% O). When particle size is evaluated at different mag-

nifications, it is established that the grain size is compatible (Fig. 2(c)).

### 3.3. EMI shielding measurements of $\text{ZnNb}_2\text{O}_6$ -chopped strands

In the range of frequency of 6.5–18 GHz, Fig. 3 demonstrates the frequency dependence of shielding effectiveness of the epoxy-chopped strands/ $\text{ZnNb}_2\text{O}_6$  composites. For SE measurements, the N 5230A PNA series network analyzer (*Agilent Technologies*) was employed. Coaxial holders with adequate diameters that preserve 50-ohm impedance at the input and output ports were used to realize SE testing. As a baseline, a value without a sample was first measured. The samples were then sequentially inserted into the apparatus, always being uniformly pinched from three distinct places to provide a consistent pressure through the sample. The apparatus sent the output values to the computer, where SE is computed. The difference between the samples' presence and absence was displayed in the computer as shielding effectiveness values. This flanged coaxial EMI SE tester is a flanged coaxial tester that maintains 50 ohm impedance over its whole length and has consistent diameters. The specimen holder is an expanded coaxial transmission line with unique taper sections and matching notches that preserve



O: wt.% 29.19; Zn: wt.% 16.88, Nb: wt.% 53.93.

Fig. 2. SEM images of single phase  $\text{ZnNb}_2\text{O}_6$  sintered for 4 h at  $1100^\circ\text{C}$  (a) at  $\times 5000$ , (b) at  $\times 10000$ , (c) EDS analysis of  $\text{ZnNb}_2\text{O}_6$  at  $\times 5000$ .

a 50 ohm characteristic impedance over the whole length of the holder [34, 35]. By repeatedly measuring specimens with a smooth, 1.5 mm-thick and a rectangular form, the device's measurement was checked. The specimen thickness is a critical dimension. For the best repeatability of SE measurements, reference specimen space and load specimen were identical in thickness, measured SE values of composites are dependent on geometry and orientation. The performance value of the shielding effect is connected to how far the incoming elec-

tromagnetic wave passes through the composite material. Among the  $\text{ZnNb}_2\text{O}_6$ -chopped strands composites, the microwave shielding efficacy of  $\text{ZnNb}_2\text{O}_6$ -chopped strands (at 60–40 wt.%) were clearly superior than those of  $\text{ZnNb}_2\text{O}_6$ -chopped strands (at 80–20 wt.%). There was just one band at 6.72 GHz with  $-51.32$  dB in  $\text{ZnNb}_2\text{O}_6$ -chopped strands compositions (at 60–40 wt.%). This composite material reaches  $-34.47$  and  $-36.25$  dB, at 11.02 and 16.55 GHz, respectively. Moreover, in the frequency regions of 6.48 and 16.89 GHz, 16.95 and



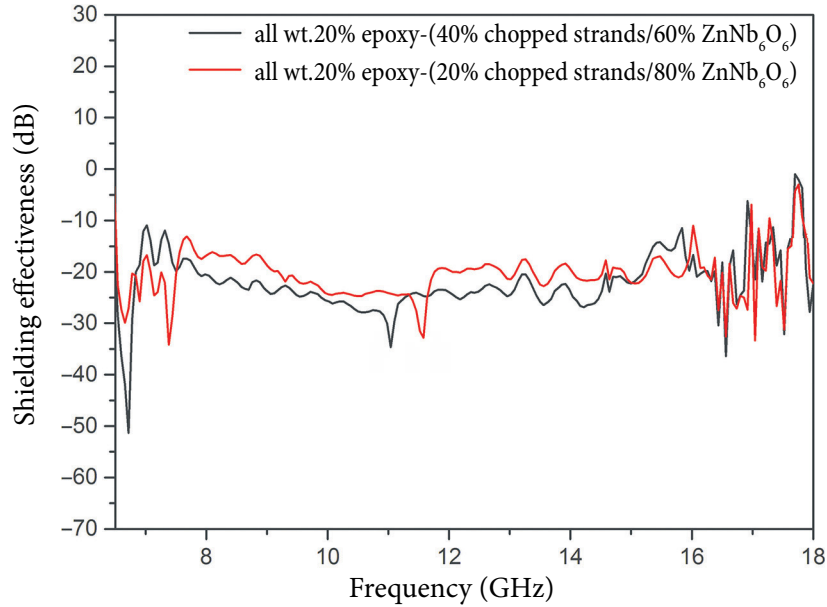


Fig. 3. Shielding effectiveness of the epoxy-(chopped strands/ $\text{ZnNb}_2\text{O}_6$ ) composites: all wt.20% epoxy-(40% chopped strands/60%  $\text{ZnNb}_2\text{O}_6$ ) compositions, all wt.20% epoxy-(20% chopped strands/80%  $\text{ZnNb}_2\text{O}_6$ ) compositions.

17.64 GHz, it achieved a shielding effectiveness below  $-10$  dB. In addition, the compositions had a shielding effectiveness below  $-20$  dB in frequency ranges of 6.5 and 6.84 GHz, 7.86 and 15.17 GHz, 17.54 and 17.88 GHz.

When the quantity of zinc niobate powder increased and the content of chopped strands dropped, the  $\text{ZnNb}_2\text{O}_6$ -chopped strands compositions (at 80–20 wt.%) reached  $-29.76$ ,  $-34.03$ ,  $-32.89$ ,  $-32.21$ ,  $-33.12$  and  $-31.1$  dB, at 6.66, 7.39, 11.56, 16.55, 17.05 and 17.52 GHz, respectively. Furthermore, this composite material showed a shielding efficacy below  $-20$  dB in frequency regions between 9.19 and 11.72 GHz, 16.65 and 16.93 GHz. In contrast, it obtained a shielding effect below  $-10$  dB in frequency ranges of 6.5 and 16.95 GHz, 17.31 and 17.66 GHz.

#### 4. Discussion

The  $\text{ZnNb}_2\text{O}_6$ -chopped strands (at 60–40 wt.%) had a better wideband shielding capability, with a value below  $-20$  dB in a frequency range of 7.86 and 15.17 GHz. The multiple reflection effect, that is caused by internal reflections in the shielding material, has an impact on EMI shielding and is most noticeable when there are plenty of big sur-

face areas or interfacial regions present in the material. These composite materials with porous structures likely have a large specific surface area and a massive interior number of grain boundaries. These properties improve the wave shielding effectiveness; also lightness of the porous structure played an important role. Interfacial polarization between chopped strands and  $\text{ZnNb}_2\text{O}_6$  plays an important role in the electromagnetic shielding material. The performance of microwave shielding effect also depends on the matching (coherence) of the impedance of irradiation on the surface of the material. Chopped strands improve the matching impedance on the transmissions between the ingredients of composites. Meanwhile, sharp shielding effect peaks appear due to the resonance effect of holder geometry and reflection.

The purpose of shielding effectiveness (SE) test is to determine the insertion loss due to introducing a material between the source and signal analyzer. There are several factors that have an impact on EMI shielding, and one of them is the reflection loss, which depends on how the mobile charge carriers (electrons or holes) interact with the incoming EM waves. The second is the absorption loss, which is affected by the interaction of magnetic and electrical dipoles with EM waves.

The third mechanism, known as the multiple reflection effect, refers to internal reflections inside the shielding material. This effect often manifests itself when there are many and sizable surface or interfacial regions. This occurrence is dependent on many reflections and refractions of electromagnetic waves, the composite's form, its microstructure and geometrical composition.

The sintered  $\text{ZnNb}_2\text{O}_6$  with porous structures likely has a large particular surface area and a massive interior number of grain boundaries. These characteristics enhance the shielding effectiveness; lightness is also a valuable property of material.

The electromagnetic shielding material greatly benefits from the interfacial polarization that occurs between chopped strands and  $\text{ZnNb}_2\text{O}_6$ . The matching (coherence) of the impedance of irradiation on the surface of the composite also affects the performance of the microwave shielding effect. Chopped semiconductor strands enhance the transmission impedance between the components of composites.

The multiinterfaces between  $\text{ZnNb}_2\text{O}_6$  powder and chopped strands stimulate the improved electromagnetic shielding effect because of the existence of interfacial polarization. There are more collisions in the surface spins when the  $\text{ZnNb}_2\text{O}_6$  crystallite size shrinks and its irregular areas expand.

The rise in the shielding effect peak widths may also be interpreted as an increase in the distribution of the observed particle size in the crystal structure.

Chopped strands based  $\text{ZnNb}_2\text{O}_6$  composites have a strong shielding effectiveness proportion for electromagnetic waves in a wide band region, and the microwave shielding action of novel composites may be modified in this technology by modifying chopped strands and  $\text{ZnNb}_2\text{O}_6$  concentration. According to studies, the concentration of chopped strands has an effect on the composite structure. The transmission of the material is influenced by chopped strands, which increases the shielding effectiveness.

## 5. Conclusions

Using the mixed oxide process,  $\text{ZnNb}_2\text{O}_6$ -chopped strands powders (at 60–40 and 80–20 wt.%, respectively) were produced. This is the first in-

vestigation of epoxy-chopped strands/ $\text{ZnNb}_2\text{O}_6$  composites that we are aware of. Controlling the chopped strands and the influence of  $\text{ZnNb}_2\text{O}_6$  powder concentration on the specimens for the required frequency ranges allows for the easy adjustment of microwave shielding means. Because of the simple and low-cost arrangement techniques and improved shielding effectiveness performance,  $\text{ZnNb}_2\text{O}_6$ -chopped strands composites have a promising future as microwave shielding effect. To improve the microwave shielding efficacy, chopped strands of  $\text{ZnNb}_2\text{O}_6$  were utilized. The most effective shielding was observed in  $\text{ZnNb}_2\text{O}_6$ -chopped strands (at 60–40 wt.%) compositions – epoxy with a minimal SE of  $-51.32$  dB at 6.72 GHz and 1.5 mm thickness. The SEM analysis corroborated the XRD result, as single phase  $\text{ZnNb}_2\text{O}_6$  in the composite. The microwave shielding features of  $\text{ZnNb}_2\text{O}_6$ -chopped strands composites show a variation depending on the amount of chopped strands. The composition of epoxy-chopped strands/ $\text{ZnNb}_2\text{O}_6$  (at 60–40 wt.%) offers a high (absolute) shielding effectiveness value of under  $-20$  dB at frequencies between 7.86 and 15.17 GHz. Between 6.48 and 16.89 GHz, this composite has a shielding effectiveness of less than  $-10$  dB. The smaller (absolute) shielding effectiveness range is provided by compositions of epoxy-chopped strands/ $\text{ZnNb}_2\text{O}_6$  (at 80–20 wt.%) with under  $-20$  dB at frequencies between 9.19 and 11.72 GHz. This composite has a shielding effect of less than  $-10$  dB in a frequency range of 6.5 to 16.95 GHz. The amount of chopped strands present has a substantial impact on shielding efficacy qualities. This type of composite was created for the first time specifically for this purpose, and the subject matter is quite limited. Microwave shielding capabilities of chopped strands based  $\text{ZnNb}_2\text{O}_6$  composites may be investigated for a larger range of constituent contributions. The  $\text{ZnNb}_2\text{O}_6$ -chopped strands composite is promising for microwave shielding throughout a broad frequency band. For future research, the synthesis of the chopped strands with  $\text{ZnNb}_2\text{O}_6$  composite can be researched in more depth with different additives and ratios. In order to improve the microwave shielding,  $\text{ZnNb}_2\text{O}_6$ -chopped strands composites are being employed. In radar frequency and higher frequency ranges, the shielding effect and reflection loss of this composite with various dopant materials might be explored.

## Acknowledgements

This work was made in honour of Prof. Dr. Ayhan Mergen, who passed away in 2017, Mr. Salim Sahin (died in 2014) and Ms. Emsal Sahin. We are very grateful to Prof. Dr. Mesut Kartal, as well as to Prof. Dr. Selcuk Paker and Prof. Dr. Sedef Kent Pinar from Istanbul Technical University. For their assistance, we also acknowledge the Advanced Technology and Application Center at Adana Alparslan Türkeş Science and Technology University.

## References

- [1] L. Zhenbau and Y. Wang, Preparation of polymer-derived graphene-like carbon-silicon carbide nanocomposites as electromagnetic interference shielding material for high temperature applications, *J. Alloys Compd.* **709**, 313–321 (2017).
- [2] A.A. Al-Ghamdi and F. El-Tantawy, New electromagnetic wave shielding effectiveness at microwave frequency of polyvinyl chloride reinforced graphite/copper nanoparticles, *Compos. A Appl. Sci. Manuf.* **41**, 1693–1701 (2010).
- [3] D. Cao, L. Pan, H. Li, J. Li, X. Wang, X. Cheng, Z. Wang, J. Wang, and Q. Liu, A facile strategy for synthesis of spinel ferrite nano-granules and their potential applications, *RSC Advances* **71**, 66795–66802 (2016).
- [4] P.F. Wilson, M.T. Ma, and J.W. Adams, Techniques for measuring the electromagnetic shielding effectiveness of materials. I. Far-field source simulation, *IEEE Trans. Electromagn. Compat.* **30**, 239–250 (1988).
- [5] E.I. Sahin and M. Emek, Electromagnetic shielding effectiveness of wollastonite/PANI/colemanite composites, *EJOSAT* **21**, 83–89 (2021).
- [6] H. Pan, X. Yin, J. Xue, L. Cheng, and L. Zhang, Microstructures and EMI shielding properties of composite ceramics reinforced with carbon nanowires and nanowires-nanotubes hybrid, *Ceram. Int.* **43**, 12221–12231 (2017).
- [7] H. Abbasi, M. Antunes, and J.I. Velasco, Recent advances in carbon-based polymer nanocomposites for electromagnetic interference shielding, *Mater. Sci.* **103**, 319–373 (2019).
- [8] A.F. Qasrawi and A.A. Hamarsheh, Structural, optical and electrical properties of band-aligned CdBr<sub>2</sub>/Au/Ga<sub>2</sub>S<sub>3</sub> interfaces and their application as band filters suitable for 5G technologies, *J. Electron. Mater.* **32**, 1–12 (2022).
- [9] S.W. Kim, Y.W. Yoon, S.J. Lee, G.Y. Kim, Y.B. Kim, Y.Y. Chun, and K.S. Lee, Electromagnetic shielding properties of soft magnetic powder-polymer composite films for the application to suppress noise in the radio frequency range, *J. Magn. Mater.* **316**, 472–474 (2007).
- [10] Y. Yuan, L. Liyang, M. Yang, T. Zhang, F. Xu, Z. Lin, Y. Ding, C. Wang, J. Li, W. Yin, Q. Peng, X. He, and Y. Li, Lightweight, thermally insulating and stiff carbon honeycomb-induced graphene composite foams with a horizontal laminated structure for electromagnetic interference shielding, *Carbon* **123**, 223–232 (2017).
- [11] X. Zhang, Y. Rao, J. Guo, and G. Qin, Multiple-phase carbon-coated FeSn<sub>2</sub>/Sn nanocomposites for high-frequency microwave absorption, *Carbon* **96**, 972–979 (2016).
- [12] S. Mondal, P. Das, S. Ganguly, R. Ravindren, S. Remanan, P. Bhawal, T.K. Das, and N.C. Das, Thermal-air ageing treatment on mechanical, electrical, and electromagnetic interference shielding properties of lightweight carbon nanotube based polymer nanocomposites, *Compos. A Appl. Sci. Manuf.* **107**, 447–460 (2018).
- [13] S. Mondal, S. Ganguly, P. Das, D. Khastgir, and N.C. Das, Low percolation threshold and electromagnetic shielding effectiveness of nanostructured carbon based ethylene methyl acrylate nanocomposites, *Compos. B Eng.* **119**, 41–56 (2017).
- [14] Y. Mu, H. Li, J. Deng, and W. Zhou, Temperature-dependent electromagnetic shielding properties of SiCf/BN/SiC composites fabricated by chemical vapor infiltration process, *J. Alloys Compd.* **724**, 633–640 (2017).
- [15] W. Lin Yao, G. Xiong, Y. Yang, H. Ging Huang, and Y. Fen Zhou, Effect of silica fume and colloidal graphite additions on the EMI shielding effectiveness of nickel fiber cement based composites, *Constr. Build. Mater.* **150**, 825–832 (2017).



- [16] H.B. Zhang, Q. Yan, W.G. Zheng, Z. He, and Z.Z. Yu, Tough graphene polymer microcellular foams for electromagnetic interference shielding, *ACS Appl. Mater. Interfaces* **3**, 918–924 (2011).
- [17] B.P. Singh, V. Choudhary, P. Saini, and R.B. Mathur, Designing of epoxy composites reinforced with carbon nanotubes grown carbon fiber fabric for improved electromagnetic interference shielding, *AIP Adv.* **2**(022151), 1–7 (2012).
- [18] G.G. Tibbetts, M.L. Lake, K.L. Strong, and B.P. Rice, A review of the fabrication and properties of vapor-grown carbon nanofiber/polymer composites, *Compos. Sci. Technol.* **67**, 1709–1718 (2007).
- [19] D.W. Kim, K.H. Ko, and K.S. Hong, Influence of copper (II) oxide additions to zinc niobate microwave ceramics on sintering temperature and dielectric properties, *J. Am. Ceram. Soc.* **84**, 1286–1290 (2001).
- [20] S.H. Wee, D.W. Kim, and S.I. Yoo, Microwave dielectric properties of low-fired  $\text{ZnNb}_2\text{O}_6$  ceramics with  $\text{BiVO}_4$  addition, *J. Am. Ceram. Soc.* **87**, 871–874 (2004).
- [21] G. Feng, L. Jiaji, H. Rongzi, L. Zhen, and T. Changsheng, Microstructure and dielectric properties of low temperature sintered  $\text{ZnNb}_2\text{O}_6$  microwave ceramics, *Ceram. Int.* **35**, 2687–2692 (2009).
- [22] L. Guo, D. Jinhui, T. Jintao, Z. Zhibin, T. He, X. Qu, and L. Zhongfang, Effects of  $\text{ZnCl}_2$  addition on the  $\text{ZnNb}_2\text{O}_6$  powder synthesis through molten salt method, *Mater. Chem. Phys.* **105**, 148–150 (2007).
- [23] H.J. Lee, I.T. Kim, and K.S. Hong, Dielectric properties of  $\text{AB}_2\text{O}_6$  compounds at microwave frequencies, *Jpn. J. Appl. Phys.* **36**, 1318–1320 (1997).
- [24] H.B. Bafrooei, E.T. Nassaj, T. Ebadzadeh, and C.F. Hu, Reaction sintering of nano-sized  $\text{ZnO-Nb}_2\text{O}_5$  powder mixture: sintering, microstructure and microwave dielectric properties, *J. Mater. Sci. Mater. Electron.* **25**, 1620–1626 (2014).
- [25] M.A. Shayed, Ch. Cherif, R.D. Hund, T. Cheng, and F. Osterod, Carbon and glass fibers modified by polysilazane based thermal resistant coating, *Text. Res. J.* **80**(11), 1118–1128 (2010).
- [26] F.M. Zhao and N. Takeda, Effect of interfacial adhesion and statistical fiber strength on tensile strength of unidirectional glass fiber/epoxy composites. Part I: experiment results, *Compos. A Appl. Sci. Manuf.* **31**, 1203–1214 (2000).
- [27] N. Gupta, T.C. Lin, and M. Shapiro, Clay-epoxy nanocomposites: Processing and properties, *JOM* **59**, 61–65 (2007).
- [28] E.İ. Şahin, M. Emek, B. Ertug, and M. Kartal, Electromagnetic shielding performances of colemanite/PANI/ $\text{SiO}_2$  composites in radar and wider frequency ranges, *BUJSE* **13**(1), 34–42 (2020).
- [29] J. Nie, G. Wang, D. Hou, F. Guo, and Y. Han, The preparation and research on the electromagnetic shielding effectiveness of T-ZnO@Ag/silicone rubber composites, *Mater. Sci.-Medzg.* **26**(2), 205–209 (2018).
- [30] B.V.S.R.N. Santhosi, K. Ramji, and N.B.R. Mohan Rao, Design and development of polymeric nanocomposite reinforced with graphene for effective EMI shielding in X-band, *Phys. B Condens. Matter* **586**, 1–9 (2020).
- [31] F. Tariq, M. Shifa, S.K. Hasan, and R.A. Baloch, Hybrid nanocomposite material for EMI shielding in spacecrafts, *Adv. Mater. Res.* **1101**, 46–50 (2015).
- [32] D.D.L. Chung, Materials for electromagnetic interference shielding, *J. Mater. Eng. Perform.* **9**, 350–354 (2000).
- [33] T.H. Ting, R.P. Yu, and Y.N. Jau, Synthesis and microwave absorption characteristics of polyaniline/NiZn ferrite composites in 2–40 GHz, *Mater. Chem. Phys.* **126**, 364–368 (2011).
- [34] S. Yang, K. Lozano, A. Lomeli, H.D. Foltz, and R. Jones, Electromagnetic interference shielding effectiveness of carbon nanofiber/LCP composites, *Compos. A Appl. Sci. Manuf.* **36**(5), 691–697 (2005).
- [35] N. Ucar, B.K. Kayaoglu, A. Bilge, G. Gurel, P. Sencandan, and S. Paker, Electromagnetic shielding effectiveness of carbon fabric/epoxy composite with continuous graphene oxide fiber and multiwalled carbon nanotube, *J. Compos. Mater.* **52**(24), 3341–3350 (2018).

## ZnNb<sub>2</sub>O<sub>6</sub> SUSMULKINTŲ GIJŲ KOMPOZITŲ ELEKTROMAGNETINIO EKSPANAVIMO EFEKTYVUMAS TAIKANT JUOS RADARUOSE IR PLATAUS (6,5–18 GHz) MIKROBANGŲ RUOŽO PRIETAISUOSE

E.İ. Şahin

*Adanos Alparslan Türkeş mokslo ir technologijų universiteto Pažangių technologijų tyrimų ir taikymo centras, Adana, Turkija*

### Santrauka

Šiame tyrime tradicinis mišraus oksido procesas buvo naudojamas ZnNb<sub>2</sub>O<sub>6</sub> susmulkintų gijų kompozitams sukurti. Vienfazis junginys, kurio cheminė formulė yra ZnNb<sub>2</sub>O<sub>6</sub>, buvo sukurtas 4 valandas sukepinus jį 1100 °C temperatūroje. Struktūriniam tyrimui buvo sukurti įvairūs ZnNb<sub>2</sub>O<sub>6</sub> susmulkintų gijų kiekiai. Struktūrinei analizei buvo atlikta rentgeno spindulių difrakcija (XRD), skenuojamoji elektronų mikroskopija (SEM) ir energijos dispersinė rentgeno spektroskopija (EDS), ir jos parodė, kad antroji ZnNb<sub>2</sub>O<sub>6</sub> fazė nesusidarė. Be to, ZnNb<sub>2</sub>O<sub>6</sub> susmulkintų gijų kompozitai buvo pagaminti karšto presavimo būdu, naudojant įvairių proporcijų ZnNb<sub>2</sub>O<sub>6</sub> susmulkintų gijų kompozicijas ir epoksidą.

ZnNb<sub>2</sub>O<sub>6</sub> susmulkintų gijų junginys įvairiais svorio santykiais ir epoksidinė derva buvo naudojami mikrobangų ekranavimo efektyvumo kompozitams gaminti. Naudojant tinklo analizatorių tirtas ZnNb<sub>2</sub>O<sub>6</sub> susmulkintų gijų kompozitų mikrobangų ekranavimo efektyvumas 6,5–18 GHz diapazone. Kai storis yra 1,5 mm, pasiekta didžiausia (pagal modulį) –51,32 dB ekranavimo efektyvumo vertė, esant 6,75 GHz. ZnNb<sub>2</sub>O<sub>6</sub> susmulkintų gijų junginiai buvo gaminami kaip kompozitai, o jų savybės apibūdintos siekiant užtikrinti ekranavimo kokybę. Komponentų proporcijos pavyzdžiuose gali būti parenkamos pritaikant juos tam tikriems dažniams ar reikalingoms dažnių juostoms, siekiant reikalingo mikrobangų ekranavimo.